RESEARCH PAPER

Development and Characterization of Naproxen-Loaded Solid Lipid Nanoparticles for Chronotherapeutic Applications

Sharad S. Kharat[1*], Moreshwar P. Patil[2]

[1,2] Department of Pharmaceutics, MET's Institute of Pharmacy, Bhujbal Knowledge City, Adgaon, Nashik – 422003, Maharashtra, India (Affiliated to Savitribai Phule Pune University, Pune, India).

[*] Equal Contribution. Corresponding Author: Sharad S. Kharat,

Email: sharad.kharat009@gmail.com, moreshwarp_iop@bkc.met.edu

Received: 28th Feb, 2026 | **Revised:** 14th Mar, 2026 | **Accepted:** 4th Apr, 2026 | **Available Online:** 20th Apr, 2026

ABSTRACT

Objective: The study aimed to develop and optimize Naproxen-loaded solid lipid nanoparticles (NAP-SLNs) using high-pressure homogenization to enhance solubility, achieve sustained drug release, and improve overall therapeutic efficacy.

Methods: A full factorial 2^3 design was employed to optimize formulation variables including lipid concentration, surfactant concentration, and homogenization cycles. Compritol ATO 888 and Poloxamer 188 were used as lipid and surfactant, respectively. The prepared SLNs were characterized for particle size, polydispersity index (PDI), zeta potential, and encapsulation efficiency (% EE). In-vitro drug release studies were conducted in phosphate buffer (pH 6.8) using a USP Type II dissolution apparatus. The optimized batch was further evaluated for stability under ICH-recommended conditions.

Results: The optimized formulation (F7) exhibited desirable physicochemical properties with a particle size of 134.5 nm, PDI of 0.351, and %EE of 89.67%. The drug release profile showed a biphasic pattern with an initial burst followed by sustained release up to 24 hours, releasing 76.02% of Naproxen. Stability studies indicated good physical and chemical stability under refrigerated conditions.

Conclusion: The developed NAP-SLNs effectively sustained drug release and demonstrated enhanced stability, making them a promising nanocarrier system for improving the oral delivery of Naproxen. This formulation could reduce dosing frequency and associated gastrointestinal side effects, contributing to better patient compliance.

Keywords: Naproxen, Solid lipid nanoparticles, High-pressure homogenization, Sustained release, Stability study.

How to cite this article: Kharat SS, Patil MP. Development and Characterization of Naproxen-Loaded Solid Lipid Nanoparticles for Chronotherapeutic Applications. Int J Drug Deliv Technol. 2026;16(30s):848-862. DOI: 10.25258/ijddt.16.30s.85

Source of support: Nil.

Conflict of interest: The authors declare no conflict of interest.

GRAPHICAL ABSTRACT

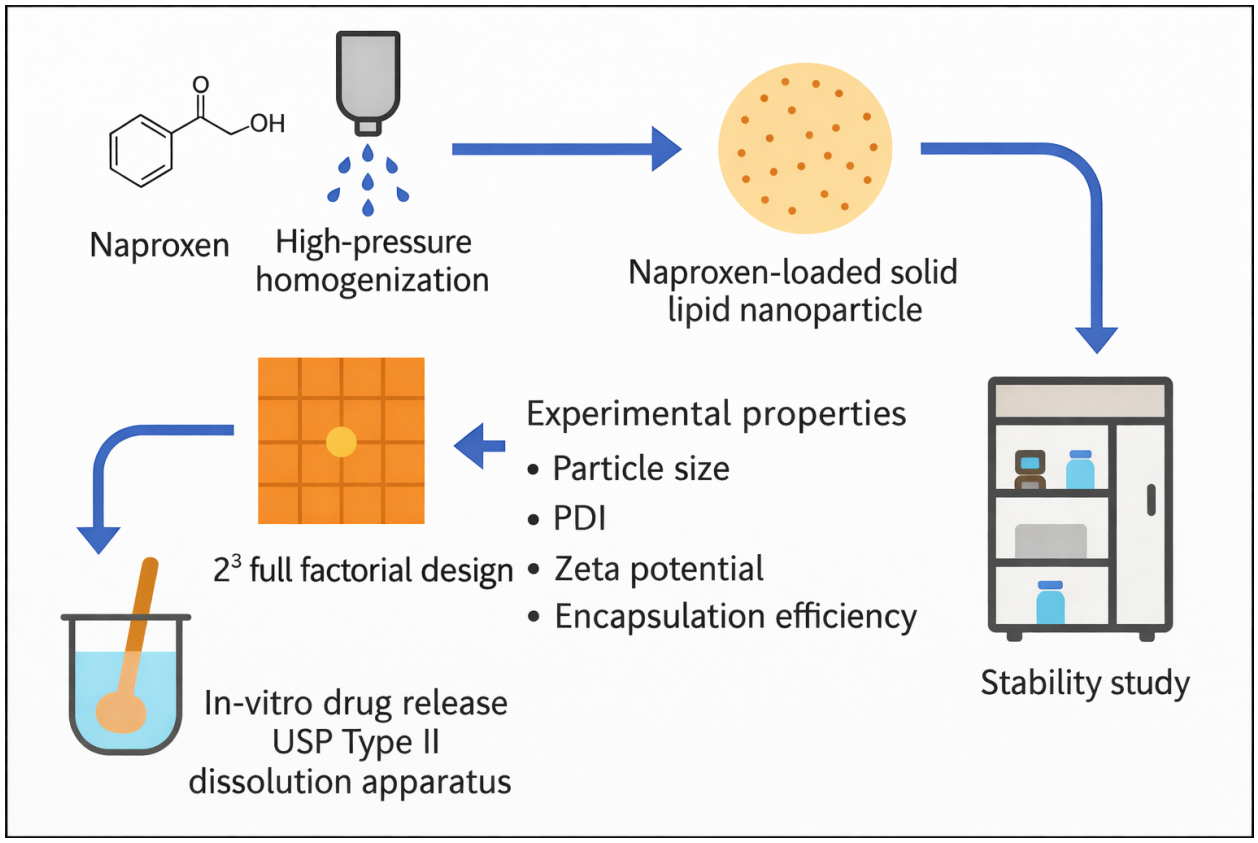

1. INTRODUCTION

Chronotherapy is an emerging paradigm in drug delivery that aligns the timing of drug administration with the body's circadian rhythms to enhance therapeutic efficacy and reduce adverse effects[1,2]. Diseases such as arthritis, asthma, cardiovascular disorders, and cancer exhibit distinct chronobiological patterns, where symptoms intensify at specific times of the day. In the context of inflammatory diseases like rheumatoid arthritis, pain and stiffness typically worsen in the early morning hours due to circadian variations in cytokine levels and prostaglandin synthesis. These observations highlight the need for drug delivery systems that can provide synchronized release profiles tailored to the body's biological clock[3].

Naproxen, a non-steroidal anti-inflammatory drug (NSAID), is widely used for the management of inflammatory conditions and pain associated with arthritis[4]. Despite its favorable pharmacodynamic profile, the conventional immediate-release formulations of naproxen are limited by their inability to maintain effective plasma concentrations at specific circadian peaks of symptoms. Moreover, repeated administration can result in gastrointestinal irritation, hepatic strain, and systemic side effects, especially when taken multiple times throughout the day. These limitations warrant the development of a delivery system capable of targeted, sustained, and time-controlled drug release[5].

Solid lipid nanoparticles (SLNs) have emerged as a versatile platform for drug delivery, offering several advantages such as biocompatibility, controlled drug release, and enhanced bioavailability. SLNs can protect labile drugs from degradation, improve drug solubility, and enable the incorporation of both hydrophilic and lipophilic drugs within a solid lipid matrix. Importantly, their nanoscale size allows for improved penetration and retention, while the lipid-based composition minimizes toxicity and facilitates large-scale production. In recent years, SLNs have gained attention for use in chronotherapeutic systems owing to their tunable release profiles and ability to sustain drug levels over extended periods [6,7].

This study focuses on the formulation and characterization of naproxen-loaded SLNs intended for chronotherapeutic application. The primary aim is to design a nanoparticulate system capable of delivering naproxen in a controlled manner, ensuring peak drug availability during early morning hours when arthritic

symptoms are most severe. The formulation process was optimized to achieve desirable physicochemical attributes, including particle size, polydispersity index, surface charge, and entrapment efficiency. Lyophilization was employed to convert the SLN suspension into a stable dry powder suitable for further development into oral solid dosage forms. *In-vitro* drug release studies were conducted to evaluate the release kinetics and potential for chronomodulated drug delivery. This work represents a step forward in the development of patient-centric therapies for inflammatory diseases, providing a robust technological foundation for future in vivo chronotherapeutic evaluation[8].

Solid lipid nanoparticles offer a unique advantage in chronotherapeutic drug delivery due to their solid lipid matrix, which allows modulation of drug diffusion and erosion kinetics. By tailoring the lipid composition and formulation parameters, SLNs can provide sustained and time-dependent drug release profiles aligned with circadian variations in disease symptoms. Such controlled release systems are particularly beneficial in inflammatory conditions like rheumatoid arthritis, where symptom severity peaks during the early morning hours, making SLNs a promising platform for chronotherapy-oriented drug delivery [9].

Furthermore, sustained release from SLNs can be strategically tailored for circadian-based dosing, such as evening administration to ensure optimal drug availability during early morning symptom exacerbation. This time-aligned release approach may enhance therapeutic outcomes while minimizing dosing frequency and adverse effects [10].

2. MATERIAL AND METHOD

Materials

Naproxen was received as a gift sample from Cipla Ltd., Mumbai, India. Compritol ATO 888 was procured from Loba Chemie Pvt. Ltd., Mumbai, India, and used as the solid lipid carrier for nanoparticle formulation. Tween 80 (pharmaceutical grade; average molecular weight ~8400 Da), serving as the surfactant, was purchased from Sigma-Aldrich, USA, while soya lecithin, used as a co-surfactant, was obtained from Central Drug House (CDH), New Delhi, India. Analytical-grade ethanol and acetone were purchased from Merck Life Science Pvt. Ltd., Mumbai, India. All other reagents and chemicals used in the study were of analytical grade. Double-distilled water was used throughout the experimental procedures.

Preparation of Naproxen-Loaded Solid Lipid Nanoparticles (SLNs)

Naproxen-loaded SLNs (NAP-SLNs) were prepared using the high-pressure homogenization (HPH) method. The aqueous phase was prepared by dissolving Tween 80 in 100 mL of double-distilled water. Separately, the organic phase was prepared by dissolving 50 mg of naproxen and a specified amount of Compritol ATO 888 in 20 mL of ethanol. This mixture was heated to 90 °C in a water bath, a temperature above the melting point of the lipid, to ensure complete dissolution of both drug and lipid[11].

The hot organic solution was slowly injected into 80 mL of the preheated aqueous phase under continuous mechanical stirring at 600 rpm using a mechanical stirrer (Remi Instruments Ltd., Mumbai, India). The emulsification process was maintained at **61 °C for 45 minutes** to form a stable coarse pre-emulsion. **This temperature was selected to maintain the lipid in a softened, semi-molten state with reduced viscosity, which facilitates efficient droplet disruption during homogenization while minimizing the risk of thermal degradation of naproxen.** The pre-emulsion was then subjected to high-pressure homogenization at 800 bar for one hour to achieve nanoparticle formation. The resulting nanoemulsion was cooled to room temperature to allow lipid recrystallization and formation of stable SLNs. The schematic representation of the formulation process is shown in Figure 1 [12].

The stirring speed of 600 rpm and emulsification time of 45 minutes were selected to provide sufficient shear for uniform dispersion of the organic phase into the aqueous phase and to ensure formation of a stable coarse emulsion before high-pressure homogenization, as reported in similar SLN preparation methods.

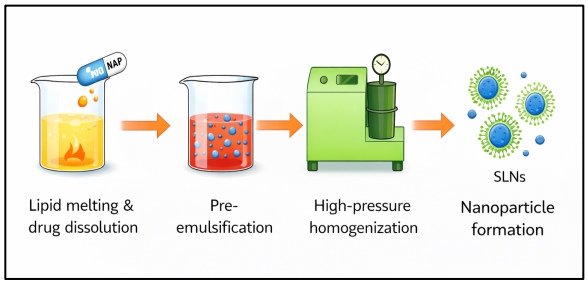

Figure 1: Schematic representation of the preparation of naproxen-loaded SLNs using high-pressure homogenization (HPH).

Experimental Design and Optimization

To optimize the SLN formulation, a full factorial 2^3 design was employed using Design-Expert software

version 8 (Stat-Ease Inc., Minneapolis, MN, USA). This statistical approach allows for the evaluation of both individual and interaction effects of selected formulation variables while minimizing the number of experimental runs required. Factorial designs are frequently used in nanoparticle optimization to generate predictive mathematical models, reduce experimental variability, and evaluate the statistical significance of factors and their interactions[13].

In this study, three independent variables were selected: lipid concentration (X_1), surfactant concentration (X_2), and homogenization pressure (X_3). Each factor was studied at two levels—low (-1) and high (+1)—as listed in Table 1. The dependent variables used for response evaluation were particle size (Y_1) and entrapment efficiency (Y_2), which are critical parameters influencing nanoparticle performance and drug delivery efficiency.

Table 1: Factorial design parameters for the preparation of naproxen-loaded SLNs.

Factors	Levels Used (Actual, Coded)
X_1 = Lipid concentration (%)	3 (−1) / 4 (+1)
X_2 = Surfactant concentration (%)	1 (−1) / 2 (+1)
X_3 = HPH pressure (bar)	800 (−1) / 900 (+1)

Coded levels represent −1 (low) and +1 (high) for statistical analysis.

Composition of Experimental Batches

Eight experimental batches of SLNs were prepared as per the factorial design. In each batch, the amount of naproxen was fixed at 50 mg, while the concentrations of lipid, surfactant, and homogenization pressure were varied according to the design matrix. A 2^3 full factorial design was employed to evaluate the main and interaction effects of formulation variables; center points were not included as response surface modeling or curvature assessment was not the objective of this study. The compositions of the eight formulations (F1–F8) are detailed in Table 2[14].

Table 2: Composition of naproxen-loaded SLNs based on factorial design.

SLN Code	X_1: Lipid (%)	X_2: Surfactant (%)	X_3: HPH Pressure (bar)
F1	3.00	2.00	800
F2	4.00	1.00	900
F3	4.00	2.00	800
F4	3.00	2.00	900
F5	4.00	1.00	800
F6	3.00	1.00	900
F7	3.00	1.00	800
F8	4.00	2.00	900

The amount of naproxen was fixed at 50 mg in all formulations.

Characterization and Evaluation of NAP-SLN Dispersion

Determination of Particle Size and Polydispersity Index (PDI)

The particle size and PDI of the NAP-SLN dispersion were determined by Dynamic Light Scattering (DLS) using a Zetasizer Nano ZS 90 (Malvern Instruments Ltd., UK). DLS measures Brownian motion and correlates it with particle size by illuminating the sample with a laser and analyzing fluctuations in scattered light intensity. All samples were diluted in a 1:10 ratio with deionized water to achieve an optimum count rate of 100–200 kilo counts per second (KCPS). Measurements were performed at 25 ± 1 °C. Measurements were conducted in triplicate, and the average particle size and standard deviation (σ) were calculated (n = 3) [15].

Zeta potential measurement

Zeta potential was measured using Laser Doppler Velocimetry (LDV) with the Zetasizer Nano ZS 90 (Malvern Instruments Ltd., UK). The electrophoretic mobility of the nanoparticles was calculated and converted to zeta potential using Henry's equation with the Smoluchowski approximation ($f(\kappa a) = 1.5$), which is applicable for aqueous dispersions of nanoparticles. Measurements were conducted in triplicate, and the average zeta potential and standard deviation (σ) were reported (n = 3)[16].

Entrapment efficiency (EE %) and drug loading (DL %)

Entrapment efficiency and drug loading were calculated by determining the concentration of unentrapped drug in the aqueous medium. Two milliliters of SLN dispersion were centrifuged at 15,000 rpm for 60 minutes at 4°C using a REMI Cooling Centrifuge (REMI Instruments Ltd., Mumbai, India). The amount of unentrapped Naproxen (NAP) in the supernatant was analyzed spectrophotometrically at 260 nm using a UV-Visible Spectrophotometer (Shimadzu UV-1800, Japan). The

EE% and DL% were calculated using the following equations[17]:

$$EE\ (\%) = \frac{Total\ drug - Free\ drug}{Total\ drug} \times 100 \quad \text{(Eq. 1)}$$

$$DL\ (\%) = \frac{Total\ NAP - Free\ NAP\ in\ supernatant}{Total\ lipid\ content} \times 100 \quad \text{(Eq. 2)}$$

Each analysis was performed in triplicate (n = 3).

Optimization of SLN formulation

Data from the above evaluations were analyzed using Design-Expert Software (Version 8.0.0; Stat-Ease Inc., Minneapolis, USA) to determine the optimized formulation.

Lyophilization of NAP-SLNs

Optimized NAP-loaded SLNs were frozen at −75°C for 24 hours with 3% w/v Mannitol as a cryoprotectant. Samples were then lyophilized for 68–72 hours using a Benchtop Freeze Dryer (Virtis SP Scientific, USA). The vials were sealed with sterile rubber closures post-lophilization[18].

Solid-state characterization

Freeze Drying of SLNs

For lyophilization study, the optimized Batch F7 was used. Different concentrations of Mannitol (2–10% w/v) were added to improve stability. Each 5 ml sample was pre-cooled at −60°C and freeze-dried at −72°C for 24 hours using a Benchtop Freeze Dryer (Virtis SP Scientific, USA; 4.5 L capacity). The dried SLNs were stored at −4°C[19].

Scanning electron microscopy (SEM)

The surface morphology of freeze-dried F7 batch was analyzed using Scanning Electron Microscope (JSM-6390, JEOL Ltd., Japan). Samples were mounted on aluminum stubs using double-sided adhesive carbon tape and sputter-coated with gold to a thickness of approximately 400 Å using a sputter coater (Quorum SC7620, UK). Imaging was performed at an accelerating voltage of 20 kV under high-vacuum conditions to examine particle morphology [20,21].

X-ray diffraction (XRD) study

Crystallinity was evaluated using an X-ray diffractometer (X'Pert Pro, PANalytical, Netherlands) equipped with a Cu Kα radiation source (λ = 1.5406 Å) and Ni filter, operating at 40 kV and 30 mA. Samples were scanned over a 2θ range of 5° to 50° at a constant scan rate of 1°/min to analyze the crystalline nature of naproxen, lipid, and NAP-SLNs [22].

Differential scanning calorimetry (DSC)

Thermal analysis was performed using a DSC instrument (Mettler Toledo®, Switzerland). Approximately 5–8 mg of sample was accurately weighed and sealed in aluminum hermetic pans, with an empty pan used as reference. Samples were heated from 40 °C to 300 °C at a rate of 10 °C/min under a nitrogen purge of 40 mL/min to observe melting and recrystallization behaviors [23].

Fourier transform infrared (FTIR) spectroscopy

Possible chemical interactions between Naproxen and Compritol ATO 888 were studied using FTIR Spectrometer (PerkinElmer Spectrum Two, USA). Spectra were recorded in the range of 4000–500 cm^{-1} at a spectral resolution of 4 cm^{-1}, with 32 scans averaged per spectrum. Spectra of pure Naproxen, Compritol ATO 888, and NAP-SLNs were compared to detect functional group changes[24].

2.6 *in-vitro* drug release study

Drug release from NAP-loaded SLNs was evaluated using the dialysis bag diffusion technique. A dialysis membrane (MWCO 100 kDa, pore size 2.4 nm) was soaked in double-distilled water overnight. Two milliliters of SLN dispersion was placed in the dialysis bag along with 2.5 mL of distilled water, sealed, and immersed in 200 mL of phosphate buffer saline (PBS, pH 6.8) maintained at 37 ± 2 °C with continuous stirring at 100 rpm. Naproxen exhibits a reported solubility of approximately 1–1.2 mg/mL in PBS pH 6.8; therefore, the selected dissolution volume ensured sink conditions throughout the study. At predetermined time intervals, aliquots were withdrawn and replaced with an equal volume of fresh PBS to maintain constant volume and sink conditions. Drug content was determined using a UV-visible spectrophotometer (Shimadzu UV-1800, Japan) at λmax 260 nm. Results were expressed as mean ± SD (n = 3) [25].

Accelerated stability study

A preliminary stability study of the lyophilized SLNs was conducted in accordance with the general principles of ICH Q1A (R2) guidelines. Samples of optimized batch F7 were packed in amber glass vials, sealed with rubber caps, and stored under refrigerated (2–8 °C) and controlled room temperature (25 ± 5 °C) conditions. Stability parameters were evaluated for a period of one month to assess short-term physical stability. [26].

3. Result and Discussion

Preparation of NAP-solid lipid nanoparticles by high pressure homogenization (HPH)

Considering the low solubility and limited gastrointestinal absorption of Naproxen (NAP), the bioavailability of the drug is restricted to approximately 58% due to its extensive hepatic first-pass metabolism.

Nanoparticle-based systems have previously been demonstrated to improve the oral bioavailability of drugs such as praziquantel, salvianolic acid, and vinpocetine. With this rationale, solid lipid nanoparticles (SLNs) were selected for the enhancement of NAP bioavailability. The proposed mechanism involves the bypassing of hepatic metabolism through lymphatic absorption.

To develop an efficient SLN formulation, several process parameters were considered. To minimize experimental runs while achieving optimization, a 2^3 full factorial design was employed. NAP-loaded SLNs were successfully prepared using a high-pressure homogenizer.

Formulation optimization of NAP-SLNs based on the factorial design (design expert software v8.0)

The factorial design included three independent variables: the concentration of Compritol ATO 888 (X1), concentration of Tween 80 (X2), and homogenization pressure (X3). The dependent variables or responses were particle size (Y1) and entrapment efficiency (Y2). The results, including polydispersity index (PDI), are summarized in Table 3 and showing in Figure 2. The statistical analysis was performed using Design-Expert software to evaluate each coefficient's significance at a 90% confidence level. Terms with a p-value less than 0.05 were considered statistically significant and included in the model.

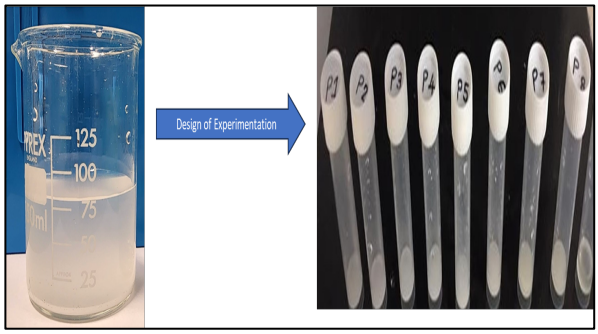

Figure 2: Figure 2: Preparation of naproxen-loaded SLNs using a DOE-based approach, illustrating hot homogenization/pre-emulsification, high-pressure homogenization, and cooling-induced lipid recrystallization for SLN formation.

Table 3: Design of formulations NAP-SLNs and results

	Factor 1	Factor 2	Factor 3	Response 1	Response2
Run	**X1:Conc.Solid lipid %**	**X2:conc.Surfactant**	**HPH pressure**	**Particale Size nm (Y1)**	**EE% (Y2)**
1	3	2	800	130	78.4
2	4	1	900	193	53.1
3	4	2	800	186	71.8
4	3	2	900	143.1	82.2
5	4	1	800	168	61.7
6	3	1	900	167.1	73.7
7	**3**	**1**	**800**	**131.1**	**89.67**
8	4	2	900	156	58.9

All values are expressed as mean ± SD (n = 3).

Optimization data analysis and model validation

A) Fitting of Data to the Model

The observed values for particle size (Y1) and entrapment efficiency (Y2) ranged from 131.1 to 193 nm and 53.1 to 89.67%, respectively. All the responses were fitted to various models using Design-Expert software, and the best-fitting models were identified for each response. The regression statistics, including R2, adjusted R2, predicted R2, standard deviation, coefficient of variation (%CV), and mean, are listed in Table 4 and 5.

During model fitting, interaction terms (AB, AC, and BC) were initially evaluated by the Design-Expert software. However, these terms were found to be statistically insignificant ($p > 0.05$) and contributed minimally to the overall model predictability. Therefore, only the significant main effects were retained in the final polynomial equations to achieve a parsimonious and statistically robust model, which is appropriate for a 2^3 full factorial design with limited experimental runs.

The predicted R^2 value for particle size (0.3286) was substantially lower than the adjusted R^2 (0.7062), indicating limited predictive capability of the model. This discrepancy may be attributed to the small number of experimental runs inherent to the 2^3 full factorial design and experimental variability associated with high-pressure homogenization. Furthermore, unaccounted process-related factors such as homogenization cycles, minor temperature fluctuations, and lipid

recrystallization behavior may have contributed to response variability.

Therefore, while the model was statistically significant (p = 0.0498) and suitable for preliminary screening of formulation variables, its predictive performance should be interpreted with caution. The optimization results should be considered indicative rather than definitive, and further validation using an expanded experimental design with additional runs is recommended to improve predictive reliability.

Table 4: Statistical summary of model fitting

Response	R^2	Adjusted R^2	Predicted R^2	SD (±)	% CV	Mean
Particle size	0.8321	0.7062	0.3286	12.40	8.13	152.54
Entrapment efficiency (%)	0.8561	0.7482	0.4245	6.26	8.80	71.18

The lower predicted R^2 for particle size may be due to limited experimental runs and process variability inherent to the 2^3 factorial design.

Table 5: ANOVA results for particle size (Y1) and EE% (Y2)

Parameter	SS	DF	MS	F-value	P-value	Model significance
Particle size (Y_1)	3048.06	3	1016.02	6.61	0.0498	Significant
Residual	614.85	4	153.71			
Entrapment efficiency (Y_2)	932.95	3	310.98	7.93	0.0369	Significant
Residual	156.79	4	39.20			

Only significant main effects (A, B, and C) were included in the final model; interaction terms were statistically insignificant (p > 0.05).

For particle size (Y_1), lipid concentration (A) showed a borderline significant effect (p = 0.0584), whereas surfactant concentration (B) and homogenization pressure (C) were not statistically significant (p > 0.05).For entrapment efficiency (Y_2), lipid concentration (A) was statistically significant (p = 0.0114), while surfactant concentration (B) and homogenization pressure (C) were not significant (p > 0.05).

Table 5a: ANOVA for individual factors

Response	Factor	SS	DF	F-value	P-value
Particle size (Y_1)	A (Lipid concentration)	2168.11	1	6.8946	0.0584
	B (Surfactant concentration)	243.10	1	0.7731	0.4289
	C (HPH pressure)	243.10	1	0.7731	0.4289
Entrapment efficiency (Y_2)	A (Lipid concentration)	769.69	1	19.6365	0.0114
	B (Surfactant concentration)	21.55	1	0.5498	0.4996
	C (HPH pressure)	141.71	1	3.6153	0.1300

A: Lipid concentration; B: Surfactant concentration; C: Homogenization pressure.F-values and p-values were calculated using a reduced linear model including only main effects in a 2^3 full factorial design. Statistical significance was considered at $p < 0.05$.

B) Effect of Independent Variables on Particle Size (Y_1)

The final reduced model equation for particle size (Y1), including only significant main effects, was: $Y_1 = 86.12500 + 22.92500A - 24.02500B + 0.20525C$ From ANOVA results, it is evident that all three independent variables significantly influenced particle size, with the p-value for the model being <0.0001. A decrease in Tween 80 concentration increased particle size due to reduced surfactant availability to stabilize the lipid dispersion. An increase in homogenization pressure effectively decreased the particle size due to the generation of high shear forces. The results suggest that higher lipid concentrations tend to increase particle size, likely due to increased viscosity and reduced efficiency of shear-induced droplet breakdown. A combination of lower lipid (3%) and surfactant (1%) concentrations with high pressure (900 bar) produced the smallest and most uniform particles. This was supported by increased PDI values at higher lipid loads, indicating aggregation due to inadequate surfactant coverage (Figure 3 to 5).

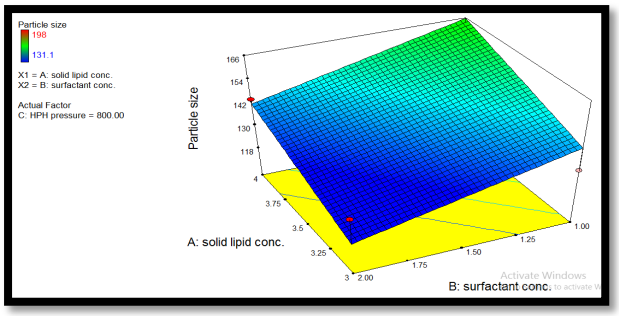

Figure 3: Response surface plot for Y1 (particle size) showing the combined effect of lipid concentration (X_1) and surfactant concentration (X_2) (AB), with homogenization pressure (X_3) held constant at the center level (850 bar).

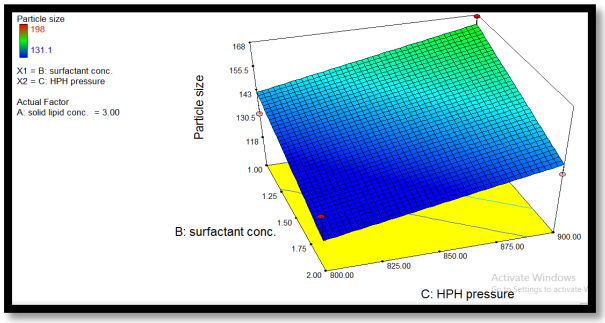

Figure 4: Response surface plot for Y1 (particle size) showing the combined effect of surfactant concentration (X_2) and homogenization pressure (X_3) (BC), with lipid concentration (X_1) held constant at the center level (3.5%).

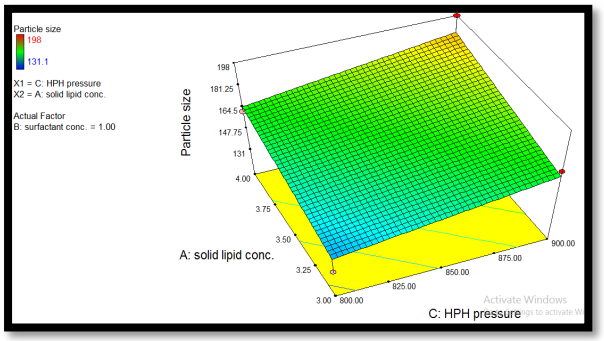

Figure 5: Response surface plot for Y1 (particle size) showing the combined effect of lipid concentration (X_1) and homogenization pressure (X_3) (AC), with surfactant concentration (X_2) held constant at the center level (1.5%).

C) Effect of Independent Variables on Entrapment Efficiency (Y2)

The final reduced model equation for entrapment efficiency (Y2) including only significant main effects, was: $Y_2 = 206.47000 - 19.61750A + 3.28250B - 0.084175C$ According to the model, the primary significant variable was lipid concentration, which negatively influenced EE%. Increasing surfactant concentration slightly improved EE due to improved stabilization of the drug-lipid matrix. However, increasing homogenization pressure had a small negative effect on EE, possibly due to thermal degradation and mechanical disruption of the lipid structure. The optimal formulation as predicted by the software used 3% Compritol ATO 888, 1% Tween 80, and a pressure of 800 bar, resulting in an experimental particle size of 131.1 nm and EE of 90%, which closely matched the predicted values (134.39 nm and 79.03%, respectively). This confirms the robustness and validity of the optimized model (Figure 6 to 8).

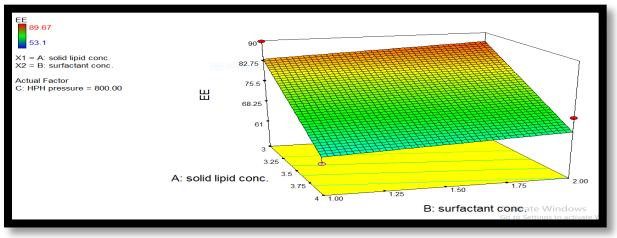

Figure 6: Response surface plot for Y2 (entrapment efficiency) showing the combined effect of lipid concentration (X_1) and surfactant concentration (X_2) (AB), with homogenization pressure (X_3) held constant at the center level (850 bar).

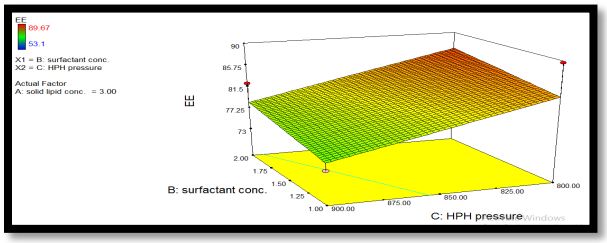

Figure 7: Response surface plot for Y2 (entrapment efficiency) showing the combined effect of surfactant concentration (X_2) and homogenization pressure (X_3) (BC), with lipid concentration (X_1) held constant at the center level (3.5%).

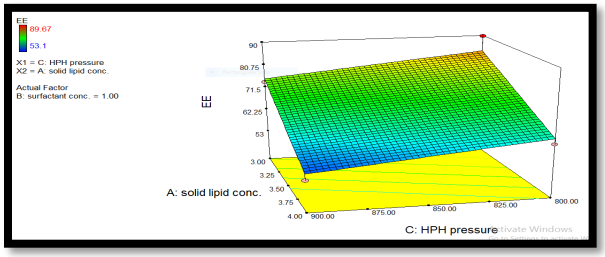

Figure 8: Response surface plot for Y2 (entrapment efficiency) showing the combined effect of lipid concentration (X_1) and homogenization pressure (X_3) (AC), with surfactant concentration (X_2) held constant at the center level (1.5%).

Characterization and evaluation of NAP-SLN dispersion

Particle Size, Polydispersity Index, and Zeta Potential

The physicochemical characteristics of Naproxen-loaded solid lipid nanoparticles (NAP-SLNs) were assessed for average particle size, polydispersity index (PDI), and zeta potential using a Zetasizer Nano ZS90 (Malvern Instruments, UK). Among the eight formulations (F1–F8), batch F7 exhibited the most favorable size distribution, with a mean particle size of 131.1 nm and a PDI of 0.351, suggesting a relatively homogeneous nanoparticle population. The zeta potential of −26.5 mV indicates moderate electrostatic repulsion, which is sufficient for physical stability despite being slightly below the ideal −30 mV threshold (Figure 8 and 10).

PDI values greater than 0.3 observed in some batches indicate a broader particle size distribution, which may lead to heterogeneous drug release behavior, with smaller particles contributing to faster initial release and larger particles sustaining prolonged release. Additionally, higher PDI values can increase the risk of particle aggregation during storage, potentially affecting physical stability and reproducibility of the formulation. Comparatively, batch F2 demonstrated the largest particle size (200 nm) and highest PDI (0.715), indicating poor stability and broad size distribution. Comparative particle size and PDI values for all batches are presented in Table 6, while representative size distribution and zeta potential profiles of the optimized batch (F7) are shown in Figures 9 and 10.

In addition to electrostatic stabilization, the presence of the non-ionic surfactant Poloxamer 188 contributes to steric stabilization by forming a hydrated polymeric layer around the nanoparticles, thereby reducing particle aggregation. Such combined electrostatic–steric stabilization is known to enhance long-term stability of lipid nanoparticles, even when zeta potential values are moderately lower than ±30 mV.

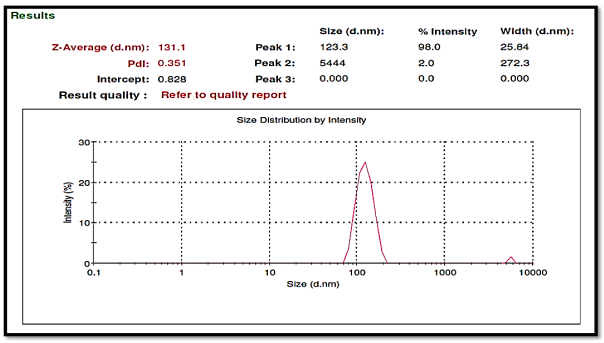

Figure 9: Particle size distribution of naproxen-loaded SLNs (batch F7) measured by dynamic light scattering, showing a mean particle size of 131.1 ± 12.4 nm and PDI of 0.351 (n = 3).

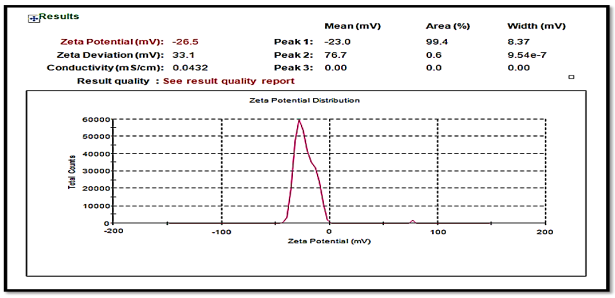

Figure 10: Zeta potential distribution of naproxen-loaded SLNs (batch F7) determined by laser Doppler velocimetry, showing a mean zeta potential of −26.5 ± 3.3 mV (n = 3).

Table 6: Evaluation of batch F1-F8.

Batch No.	Particle size (nm)	PDI
F1	140.0	0.798
F2	200.0	0.715
F3	147.0	0.273
F4	138.1	0.524
F5	168.0	0.358
F6	164.1	0.282
F7	131.0	0.351
F8	148.0	0.244

PDI denotes polydispersity index; values greater than 0.3 indicate a broad particle size distribution.

Entrapment efficiency and drug loading

Entrapment efficiency (EE%) and drug loading (DL%) were determined for all formulations. After ultracentrifugation of the SLN dispersion at 15,000 rpm for 60 minutes at 4°C using a Remi C-24BL cooling centrifuge, the supernatant was analyzed using a UV-Visible spectrophotometer (Shimadzu UV-1800, Japan) at 260 nm to quantify free drug. Batch F7 showed the

highest EE of 89.67% and a DL of 14.32%, confirming effective drug incorporation into the lipid matrix. The high EE is attributable to optimized lipid–surfactant ratios and processing conditions, while the moderate DL is consistent with the solubility limits of Naproxen in the lipid core.

Effect of formulation parameters

Formulation variables including lipid concentration, surfactant level, and homogenization pressure significantly influenced the nanoparticle characteristics. Increasing lipid concentration led to larger particle sizes due to elevated viscosity and restricted dispersion. Conversely, optimized homogenization pressure (800 bar) and 1% Tween 80 enabled reduction in size and improved stability. The selected F7 batch, with 3% Compritol ATO 888, 1% Tween 80, and high-pressure homogenization at 800 bar, was identified as the optimal formulation based on balanced particle size, PDI, and entrapment.

Freeze-drying and redispersibility

To enhance long-term storage stability, the optimized SLNs were freeze-dried using a LabconcoFreeZone 2.5 benchtop lyophilizer (USA) at −75°C under a vacuum pressure of 76 mTorr for 72 hours. Mannitol was evaluated as a cryoprotectant at 2%, 3%, and 5% w/v. The formulation with 3% mannitol produced a dry, free-flowing lyophilized cake that redispersed uniformly upon rehydration. Lower mannitol concentration (2%) resulted in a sticky, collapsed matrix, while 5% offered no added benefit. Therefore, 3% mannitol was selected for final formulation and further physicochemical and *in-vitro* evaluations.

Solid state characterization of optimized SLNs

Differential scanning calorimetry (DSC)

Differential Scanning Calorimetry analysis was performed using a DSC instrument (Model: Mettler Toledo DSC 1) to assess the physical state of Naproxen (NAP) in the solid lipid nanoparticles (SLNs). The thermogram of pure NAP exhibited a sharp endothermic melting peak at approximately 220°C, indicative of its crystalline nature. Compritol ATO 888, the lipid matrix, showed a distinct melting peak around 71°C. In contrast, the DSC thermogram of lyophilized NAP-SLNs (F7 batch) did not display the melting peak of NAP, confirming the successful encapsulation and conversion of the drug from a crystalline to an amorphous state within the lipid matrix (Figure 11).

The conversion of naproxen to an amorphous state is advantageous for enhancing apparent solubility and dissolution rate, as amorphous forms possess higher free energy and reduced lattice strength compared to crystalline counterparts. However, amorphous systems are thermodynamically unstable and may undergo recrystallization during storage, potentially affecting long-term stability. In the present formulation, the solid lipid matrix and steric stabilization provided by surfactants are expected to restrict molecular mobility and reduce the likelihood of recrystallization, although extended stability studies are required to confirm long-term physical stability.

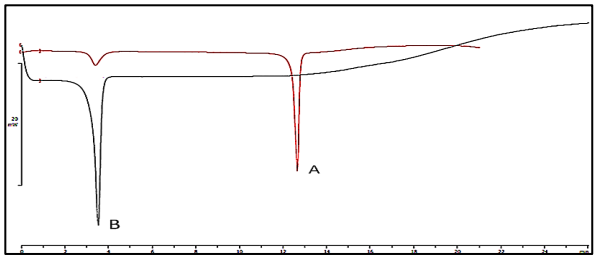

Figure 11: DSC Overlay of A) NAP-SLNs (F7), B) CompritolATO888

Fourier transform infrared spectroscopy (FTIR)

FTIR spectroscopy was carried out using a Bruker Alpha II FTIR spectrometer to investigate the possible interactions between NAP and Compritol ATO 888 in the SLN formulation. The spectrum of NAP-SLNs exhibited broad O-H stretching at 3302.85 cm^{-1}, characteristic C-H aromatic stretching at 3080.09 cm^{-1}, and CH_2 stretching vibrations at 2921.28 and 2871.14 cm^{-1}, indicative of the lipid matrix. The prominent C=O stretching at 1733.99 cm^{-1} suggested the presence of ester groups from Compritol ATO 888, while peaks at 1638.38 and 1261.06 cm^{-1} were related to aromatic C=C and C-O stretches of Naproxen. These findings confirm the encapsulation of the drug within the lipid matrix and suggest molecular interactions contributing to stability and modified release behavior (Figure 12; Table 7).

Table 7: FTIR Peak Values for Naproxen and Compritol ATO 888 in NAP-SLNs

Peak (cm^{-1})	Assignment	Component
3302.85	O-H stretching	Naproxen, Compritol ATO 888
3080.09	C-H aromatic stretching	Naproxen
2921.28	CH_2 asymmetric stretching	Compritol ATO 888
2871.14	CH_2 symmetric stretching	Compritol ATO 888

1733.99	C=O stretching	Compritol ATO 888
1638.38	C=C stretching	Naproxen
1462.70	CH_2 bending	Compritol ATO 888
1261.06	C-O stretching	Compritol ATO 888
1104.28	C-O stretching in alcohols and carboxylic acids	Naproxen, Compritol ATO 888
947.94	Out-of-plane bending of aromatic C-H bonds	Naproxen
847.74	C-H bending in aromatic rings	Naproxen
660.43	Aromatic C-H bending	Naproxen
532.26	Bending vibrations in long-chain hydrocarbons	Compritol ATO 888

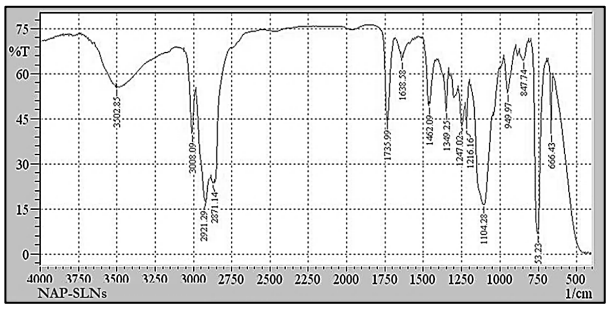

Figure 12: FTIR Peak Values for Naproxen and Compritol ATO 888 in NAP-SLNs

Scanning electron microscopy (SEM)

The surface morphology of optimized NAP-SLNs (F7 batch) was visualized using Scanning Electron Microscopy (SEM, Model: JEOL JSM-IT300). SEM images revealed rod-shaped nanoparticles, with notable aggregation likely caused by the lyophilization process. The particle size observed via SEM was relatively larger than that measured by dynamic light scattering, further indicating aggregation during freeze-drying (Figures 13 and 14).

Such aggregation is commonly observed in freeze-dried nanoparticulate systems due to ice crystal formation and close particle contact during solvent sublimation. However, this aggregation is often reversible upon reconstitution, particularly in the presence of surfactants such as Poloxamer 188, which facilitate redispersion by steric stabilization. Although partial aggregation may influence initial redispersion behavior, it is not expected to adversely affect in-vivo performance, as the nanoparticles are likely to redisperse under physiological conditions following oral administration.

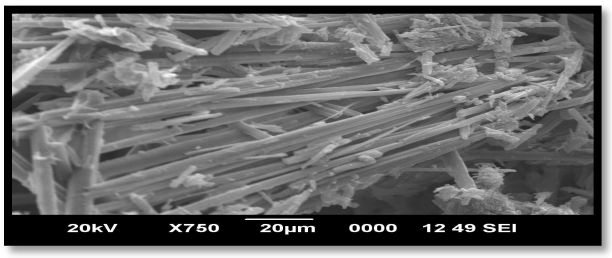

Figure 13: SEM image of optimized naproxen-loaded SLNs (batch F7) showing particle morphology at 50,000× magnification. The observed aggregation is likely induced during the lyophilization process. Scale bar: 500 nm.

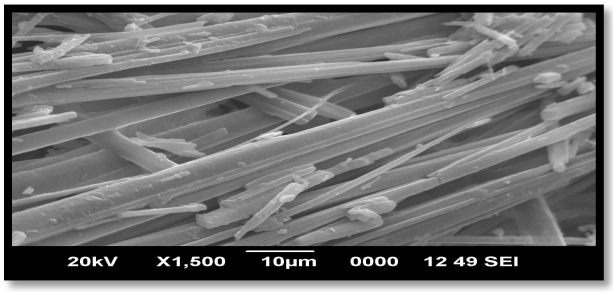

Figure 14: SEM image of optimized naproxen-loaded SLNs (batch F7) at higher resolution (50,000× magnification), illustrating particle aggregation attributed to freeze-drying. Scale bar: 500 nm.*X-Ray Diffraction (XRD)*

XRD analysis was conducted using a Bruker D8 Advance X-ray diffractometer to assess the crystalline characteristics of pure NAP and the lyophilized NAP-SLNs. The XRD pattern of pure Naproxen showed distinct sharp peaks at 2θ values such as 8.91°, 9.52°, 12.03°, 14.68°, and 20.66°, consistent with its crystalline structure. In contrast, the XRD pattern of NAP-SLNs revealed significant changes, including reduced intensity and altered peak positions. The most intense peak at 2θ = 19.89° had a d-spacing of 4.45856 and intensity of 1687 counts (100%), highlighting the dominant amorphous nature of the encapsulated drug. The absence of several crystalline peaks of pure NAP in the SLN formulation suggests a molecularly dispersed, amorphous drug state within the lipid matrix, which may contribute to

enhanced solubility and bioavailability (Figure 15; Table 8).

The degree of crystallinity of naproxen in SLNs was estimated using a relative crystallinity approach based on the ratio of characteristic peak intensities. Compared to pure naproxen (considered as 100% crystalline), the relative crystallinity of naproxen in the SLN formulation was reduced to approximately 30–35%, confirming substantial amorphization following encapsulation. The reduction in crystallinity supports the DSC findings and suggests improved molecular dispersion of naproxen within the solid lipid matrix, which may contribute to enhanced solubility and dissolution behavior.

Table 8: X-Ray diffraction data of NAP-SLNs

Caption	Angle	d value	Intensity count	Intensity (%)
d=19.57949	4.509	19.57949	225	13.3
d=9.29990	9.502	9.29990	248	14.7
d=8.03896	10.997	8.03896	196	11.6
d=6.45622	13.705	6.45622	665	39.4
d=5.11359	9.761	5.11359	1552	92
d=4.69562	18.884	4.69562	321	19
d=4.45856	**19.898**	**4.45856**	**1687**	**100**
d=4.33642	20.464	4.33642	1614	95.6
d=4.14681	21.411	4.14681	919	54.5
d=3.23067	27.588	3.23067	257	15.2
d=2.05696	43.985	2.05696	181	10.7

Relative crystallinity was estimated based on the reduction in characteristic peak intensities compared to pure naproxen.

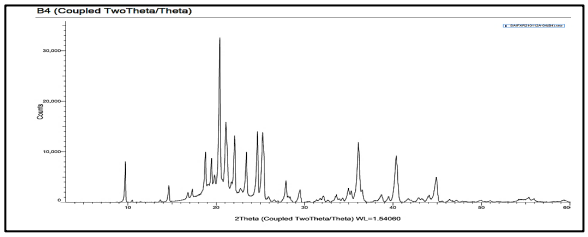

Figure 15: The X-Ray diffractogram of NAP-SLNs

***In-vitro* drug release study of NAP-SLNs**

The in-vitro drug release profile of the optimized NAP-SLNs (batch F7) was evaluated for a total duration of 24 hours using a USP Type II dissolution apparatus (paddle method, Electrolab, India) in phosphate buffer (pH 6.8) maintained at 37 ± 0.5 °C. Samples were withdrawn at predetermined time intervals (0.5, 1, 2, 4, 6, 8, 10, and 24 h) and analyzed at 271 nm using a UV-visible spectrophotometer (Shimadzu UV-1900).

The optimized SLNs exhibited a biphasic drug release pattern, characterized by an initial release of approximately 10.31% within the first 2 hours, followed by a sustained release phase extending up to 24 hours. The initial release may be attributed to drug adsorbed on or near the nanoparticle surface, whereas the prolonged release phase is likely governed by diffusion of naproxen through the Compritol ATO 888 lipid matrix and gradual matrix erosion.At 10 hours, the cumulative drug release from SLNs was 65.71%, whereas plain naproxen suspension exhibited rapid release of approximately 83.37% within the same period. The cumulative release from NAP-SLNs reached 76.02% at 24 hours, indicating effective retardation of drug release compared to the suspension (Table 9; Figure 16).

From a chronotherapeutic perspective, inflammatory conditions such as rheumatoid arthritis exhibit circadian variation, with peak symptom severity occurring during the early morning hours (approximately 4–8 AM). If the optimized formulation is administered in the evening (e.g., 8–10 PM), the gradual release profile would allow drug levels to increase progressively during the night, with approximately 25.84% release at 6 hours and 45.48% release at 8 hours. This corresponds to the early-morning symptom peak, suggesting potential suitability of the formulation for evening dosing aimed at improved morning symptom control. The sustained release up to 24 hours may further help maintain therapeutic drug levels

throughout the following day. However, in vivo pharmacokinetic studies are required to confirm the chronotherapeutic advantage of the developed formulation.

Table 9: *In-vitro* release profile of NAP suspension and NAP-SLNs

Time (hr)	NAP-suspension	NAP-SLN
0	0	0
1	10.34 ± 7.8	4.12 ± 0.688
2	12.76 ± 1.23	10.31 ± 0.997
3	20.97 ± 1.24	13.34 ± 1.02
4	25.45 ± 1.11	18.97 ± 1.11
5	33.58 ± 0.989	22.61 ± 0.9795
6	40.56 ± 2.11	25.84 ± 2.188
7	54.92 ±1.34	37.72± 1.18
8	63.98 ± 0.51	45.48 ± 1.51
9	67.01 ± 3.56	52.12 ± 1.79
10	83.37 ± 2.31	65.71 ± 0.98
24	…..	76.02 ± 1.33

Data are expressed as mean ± SD (n = 3).

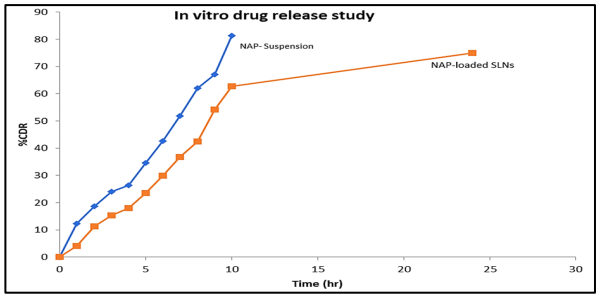

Figure 16. In vitro drug release profile of naproxen suspension and naproxen-loaded solid lipid nanoparticles (SLNs) in PBS pH 6.8 at 37 ± 0.5 °C (n = 3). Naproxen suspension showed rapid release within 10 h, whereas SLNs exhibited sustained release up to 24 h.

Release Kinetic Modeling

To elucidate the drug release mechanism, the in-vitro release data of optimized NAP-SLNs (batch F7) were fitted to various kinetic models, including zero-order, Higuchi, and Korsmeyer–Peppas models. The regression analysis indicated that the Higuchi model provided the best fit, suggesting diffusion-controlled drug release from the solid lipid matrix. The Korsmeyer–Peppas model yielded a release exponent (n) value between 0.45 and 0.89, indicating a non-Fickian (anomalous) transport mechanism involving a combination of diffusion and lipid matrix erosion. These findings support the observed biphasic release pattern, characterized by an initial burst release followed by sustained drug release.

Table 9a: Kinetic modeling of in-vitro drug release from NAP-SLNs (F7)

Kinetic model	Release mechanism	Regression coefficient (R^2)
Zero-order	Concentration-independent release	—
Higuchi	Diffusion-controlled release	Highest
Korsmeyer–Peppas	Anomalous (diffusion + erosion)	(n = 0.45–0.89)

n is the release exponent indicating the drug release mechanism.

Accelerated stability of optimized NAP–SLNs

A one-month preliminary stability study of the optimized naproxen-loaded SLNs was conducted under refrigerated (2–8 °C) and controlled room temperature (25 ± 5 °C) conditions. Key parameters including particle size, polydispersity index (PDI), and encapsulation efficiency (%EE) were evaluated at initial time and after one month of storage.

At baseline, the formulation exhibited a particle size of 134.5 nm, PDI of 0.351, and %EE of 89.67%. After one month of storage at 25 ± 5 °C, particle size increased to 167.3 nm, with a reduction in %EE to 77.4% and a slight increase in PDI (0.385). Under refrigerated conditions, comparatively smaller changes were observed, with particle size increasing to 142.8 nm, %EE decreasing to 83.6%, and PDI remaining relatively stable (0.367), as shown in Table 10.

Due to the preliminary nature of the one-month stability assessment and limited replicate data (n = 3), the observed changes are presented descriptively. Although variations were noted, particularly under room temperature conditions, refrigerated storage demonstrated comparatively better short-term stability. However, longer-term stability studies with larger sample sizes and statistical validation are required to confirm the significance of these changes.

Table 10. Preliminary stability data of optimized NAP-SLNs after One-month preliminary storage (mean ± SD, n = 3).

Storage Condition	Sampling Time (months)	Particle Size (nm)	PDI	Encapsulation Efficiency (% EE)
At time of preparation	Initial	134.5	0.351	89.67
Refrigerated (2-8°C)	1	142.8	0.367	83.6
Accelerated (25°C ± 5°C)	1	167.3	0.385	77.4

Values are expressed as mean ± SD (n = 3). Stability evaluation represents a preliminary one-month study conducted in accordance with the general principles of ICH Q1A (R2) guidelines.

CONCLUSION

The present study successfully developed and optimized Naproxen-loaded solid lipid nanoparticles (NAP-SLNs) using high-pressure homogenization to enhance the drug's bioavailability and sustain its release. Among the prepared batches, formulation F7 demonstrated optimal characteristics, including minimal particle size (134.5 nm), narrow PDI (0.351), and high encapsulation efficiency (89.67%). Design-Expert software effectively guided the optimization process through a 2^3 Full Factorial Design, confirming the significance of formulation variables via ANOVA and model validation. *In-vitro* drug release studies revealed a biphasic and sustained release pattern extending over 24 hours, with NAP-SLNs exhibiting prolonged drug release compared to plain suspension. One-month preliminary stability study conducted per ICH guidelines, confirmed that the formulation remains physically and chemically stable under cold storage conditions, with minor changes in particle size and encapsulation efficiency. Overall, the developed NAP-SLNs present a promising nanocarrier system for enhancing the therapeutic performance of Naproxen by improving its solubility, prolonging release, and potentially minimizing dosing frequency and gastrointestinal side effects. Future *in-vivo* evaluations will further establish their clinical applicability for controlled drug delivery.

ACKNOWLEDGMENTS

The authors acknowledge the use of AI-assisted language editing tools for grammatical refinement and structural organization of the manuscript. No AI tools were used for data generation, statistical analysis, interpretation of results, or scientific decision-making. All experimental work, data analysis, and conclusions were performed solely by the authors.

CONFLICT OF INTEREST

The authors declare that there is no conflict of interest.

FUNDING

The authors declare that no funding was received for the preparation of this review article.

AUTHOR CONTRIBUTIONS

Mr. Sharad S. Kharat*: Conceptualization, Methodology, Investigation, Data Curation, Formal Analysis, Writing – Original Draft, Visualization, and Supervision.***Dr. Moreshwar P. Patil***: Validation, Resources, Data Analysis, Writing – Review & Editing, Project Administration, Funding Acquisition, Technical Guidance, and Final Approval of the Manuscript.

ABBREVIATIONS

ANOVA: Analysis of variance, **EE**%: Entrapment efficiency, **HPMC**: Hydroxypropyl methylcellulose, **ICH**: International Council for Harmonisation, **NAP-SLNs**: Naproxen-loaded solid lipid nanoparticles, nm: Nanometer, **PB**: Phosphate buffer, **PDI**: Polydispersity index, rpm: Revolutions per minute, **SD**: Standard deviation, **SLNs**: Solid lipid nanoparticles, **USP**: United States Pharmacopeia, **UV**: Ultraviolet

REFRANCES

1. Lévi F. Circadian chronotherapy for human cancers. Lancet Oncol. 2001;2(5):307–315.
2. Cardinali DP, Brown GM, Pandi-Perumal SR. Chronotherapy. Handb Clin Neurol. 2021;179:357–370.
3. Ursini F, De Giorgi A, D'Onghia M, De Giorgio R, Fabbian F, Manfredini R. Chronobiology and chronotherapy in inflammatory joint diseases. Pharmaceutics. 2021;13(11):1832.
4. Davies NM, Anderson KE. Clinical pharmacokinetics of naproxen. Clin Pharmacokinet. 1997;32(4):268–293.
5. Day RO, Graham GG. Non-steroidal anti-inflammatory drugs (NSAIDs). BMJ. 2013;346:f3195.
6. Tapeinos C, Battaglini M, Ciofani G. Advances in the design of solid lipid nanoparticles and nanostructured lipid carriers for targeting brain diseases. J Control Release. 2017;264:306–332.

7. Mehnert W, Mäder K. Solid lipid nanoparticles: Production, characterization and applications. Adv Drug Deliv Rev. 2012;64 Suppl:83–101.
8. Albuquerque T, Neves AR, Faria R, Quintela T, Costa D. Chronobiology and nanotechnology for personalized cancer therapy. Cancer Nanotechnol. 2023;14:205–227.
9. Priyanka P, Rekha MS, Devi AS. Review on formulation and evaluation of solid lipid nanoparticles for vaginal application. Int J Pharm Pharm Sci. 2022;14(1):1–8.
10. Jaiswal PK, Keserwani S, Chakrabarty T. Lipid-polymer hybrid nanocarriers as a novel drug delivery platform. Int J Pharm Pharm Sci. 2022;14(4):1–12.
11. Thatipamula RP, Palem CR, Gannu R, Mudragada S, Yamsani MR. Formulation and in vitro characterization of domperidone loaded solid lipid nanoparticles and nanostructured lipid carriers. Daru. 2011;19(1):23–32.
12. Priyanka K, Abdul Hasan Sathali A. Preparation and evaluation of montelukast sodium loaded solid lipid nanoparticles. J Young Pharm. 2012;4(3):129–137.
13. Hao J, Wang F, Wang X, Zhang D, Bi Y, Gao Y, et al. Development and optimization of baicalin-loaded solid lipid nanoparticles prepared by coacervation method using central composite design. Eur J Pharm Sci. 2012;47(2):497–505.
14. Zhang J, Fan Y, Smith E. Experimental design for the optimization of lipid nanoparticles. J Pharm Sci. 2009;98(5):1813–1819.
15. Danaei M, Dehghankhold M, Ataei S, Hasanzadeh Davarani F, Javanmard R, Dokhani A, et al. Impact of particle size and polydispersity index on the clinical applications of lipidic nanocarrier systems. Pharmaceutics. 2018;10(2):57.
16. Freitas C, Müller RH. Effect of light and temperature on zeta potential and physical stability in solid lipid nanoparticle dispersions. Int J Pharm. 1998;168(2):221–229.
17. Song X, Zhao Y, Hou S, Xu F, Zhao R, He J, et al. Dual agents loaded PLGA nanoparticles: Systematic study of particle size and drug entrapment efficiency. Eur J Pharm Biopharm. 2008;69(2):445–453.
18. Howard MD, Lu X, Jay M, Dziubla TD. Optimization of the lyophilization process for long-term stability of solid-lipid nanoparticles. Drug Dev Ind Pharm. 2012;38(10):1270–1279.
19. Schwarz C, Mehnert W. Freeze-drying of drug-free and drug-loaded solid lipid nanoparticles. Int J Pharm. 1997;157(2):171–179.
20. Dubes A, Parrot-Lopez H, Abdelwahed W, Degobert G, Fessi H, Shahgaldian P, et al. Scanning electron microscopy and atomic force microscopy imaging of solid lipid nanoparticles derived from amphiphilic cyclodextrins. Eur J Pharm Biopharm. 2003;55(3):279–282.
21. Hatziantoniou S, Deli G, Nikas Y, Demetzos C, Papaioannou GT. Scanning electron microscopy study on nanoemulsions and solid lipid nanoparticles containing high amounts of ceramides. Micron. 2007;38(8):819–823.
22. Andonova V, Peneva P. Characterization methods for solid lipid nanoparticles (SLN) and nanostructured lipid carriers (NLC). Curr Pharm Des. 2017;23(43):6630–6642.
23. Castelli F, Puglia C, Sarpietro MG, Rizza L, Bonina F. Characterization of indomethacin-loaded lipid nanoparticles by differential scanning calorimetry. Int J Pharm. 2005;304(1–2):231–238.
24. Gaffney JS, Marley NA, Jones DE. Fourier transform infrared (FTIR) spectroscopy. In: Characterization of Materials. Hoboken (NJ): Wiley; 2012. p. 1–33.
25. Harivardhan Reddy L, Vivek K, Bakshi N, Murthy RSR. Tamoxifen citrate loaded solid lipid nanoparticles (SLN): Preparation, characterization, in vitro drug release, and pharmacokinetic evaluation. Pharm Dev Technol. 2006;11(2):167–177.
26. Zielińska A, Ferreira NR, Feliczak-Guzik A, Nowak I, Souto EB. Loading, release profile and accelerated stability assessment of monoterpenes-loaded solid lipid nanoparticles. Pharm Dev Technol. 2020;25(7):832–844.